Chapter 9

AERODYNAMIC PERFORMANCE ANALYSIS

An aerodynamic performance analysis is essential for nearly all aspects of axial-flow compressor aerodynamic design and application. There are basically two types of performance analysis techniques in common use: One-dimensional or mean-line methods analyze the performance along a mean stream surface. If applied to well-designed stages, the mean-line performance may be considered to be representative of the overall performance, at least near the compressor's design operating conditions. This approach is more questionable for off-design performance prediction. In those cases, blade incidence angle matching, blade loading levels, etc., may vary dramatically at different locations along the blade span, such that the mean-line performance is no longer representative of the overall performance. This is particularly true with respect to blade loading limits, blade stall and end-wall stall, which establish the compressor's surge limit. In off-design operation, the extremes in incidence angle and flow diffusion will almost always occur on the hub or the shroud contours. Some one-dimensional methods include approximate calculations at the hub-and-shroud contours to provide additional guidance to the user and to better evaluate tip clearance losses, shroud leakage effects and end-wall boundary layer blockage. The more general approach is to conduct the performance analysis for a series of stream surfaces from hub to shroud. These methods are referred to by various names, such as streamline methods, through-flow methods, streamline-curvature methods or three-dimensional methods. Hub-to-shroud performance analysis is a more accurate term, which is used in this book. It has been common practice to conduct hub-to-shroud performance analysis using the full normal equilibrium equation as described in Chapter 7. The longer computer times required and reduced reliability due to numerical instability for these techniques is probably the main reason that one-dimensional methods have continued to be used. But if the through-flow analysis offers the approximate normal equilibrium models described in section 7.6, the advantages of a hub-to-shroud performance analysis can be obtained with computation speed and reliability comparable to those of a mean-line method. Consequently, there is really no longer a need for one-dimensional performance analysis methods for axial-flow compressors.

The component parts of a hub-to-shroud performance analysis have been presented in Chapters 6 to 8. This chapter describes methods to integrate those component analyses into a hub-to-shroud performance analysis and suggests some

useful features that can make it more effective. It also compares performance predictions from this performance analysis against experimental data for axial-flow compressors to demonstrate the merits of the procedures presented in Chapters 6 to 8.

NOMENCLATURE

A_R = diffuser area ratio
b = diffuser passage width
c = blade chord length
D_{eq} = equivalent diffusion factor
g = staggered spacing
i = stream surface number
L = diffuser or camberline length
N = number of stream surfaces
P = pressure
r = radius
s = cascade pitch
t_b = blade maximum thickness
V_R = diffuser velocity ratio
W = relative velocity
W_{RE} = equivalent velocity ratio
Z = number of blades
z = axial coordinate
γ = stagger angle
θ = camber angle
κ = blade camberline angle
σ = solidity
ϕ = stream surface slope angle
$\overline{\omega}$ = total pressure loss coefficient

Subscripts

c = corrected (smoothed) parameter
t = total thermodynamic condition
1 = inlet condition
2 = discharge condition

Superscripts

$'$ = relative condition

9.1 GEOMETRY CONSIDERATIONS

Application of procedures from previous chapters requires specific procedures for specifying the geometry of the end-wall contours, quasi-normals and blades

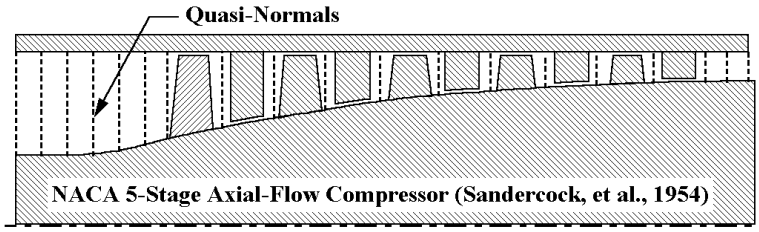

FIGURE 9-1 Basic Gas Path Geometry for an Axial-Flow Compressor

in a form suitable for the performance analysis. Figure 9-1 illustrates the basic gas path geometry for a typical axial-flow compressor. The hub-and-shroud contour coordinates are entered at the end points of a series of quasi-normals that are used to conduct the analysis. In this example, all quasi-normals are simple radial lines, although that is certainly not a requirement. This analysis used a single quasi-normal between successive blade rows, although more could have been used if they were considered necessary. For each quasi-normal after the first one, it is necessary to specify what type of blade row lies upstream. Some choices for this specification are rotor, stator, guide vane or none. It is useful to distinguish between stators and guide vanes so that the analysis can correctly distinguish stages by stage number to permit individual stage performance data to be output. The end-wall contour specification should also identify the first and last quasi-normals for which the hub wall is rotating, so that the end-wall boundary layer analysis can use the correct wall rotation speed. In this case, that is simply the first and last quasi-normal. It is also useful to provide for alternate input to size the annulus. In that case, coordinates are specified for only one end-wall contour. The angle between the quasi-normal and a radial line and the meridional velocity for the mean streamline are the other data required. The program will then compute the annulus area required and the coordinates of the other end-wall as outlined in Chapter 7.

The blade geometry also needs to be specified. The standard blade profile types described in Chapter 4 should be available to make full use of the empirical blade performance models of Chapter 6. The blade construction logic of Chapter 4 is recommended so that the blade throat openings can be computed accurately. Alternatively, the empirical approximation of Eq. (4-31) can be used, although the more precise calculation is preferred. When the latter approach is used, provision should be made to compute the throat openings one time and save the computation in the program's input file once all other blade geometry is available. It is inefficient to have the program perform these calculations every time a performance analysis is conducted. If a special blade profile such as a controlled diffusion airfoil is in use, it will be necessary to extend the methods of Chapters 4 and 6, or to confirm that use of one of the standard profiles can adequately approximate the performance of the profile. Usual practice is to specify the geometry of blade sections at a series of radii that extend over a range at least as large as the range of end-wall radii at the quasi-normals before and after the blade row. Usually it is reasonable to specify a single value of the location of the point of maximum camber, a / c, for each blade row. Similarly, a single specification per blade row can be

supplied for the number of blades in the blade row, Z, and the blade tip clearance, δ_c. The most useful data to supply for the radial sections are the chord, c, the thickness-to-chord ratio, t_b / c, and the blade inlet and discharge angles, κ_1 and κ_2. For double-circular-arc blades, a specification for the leading and trailing edge radii may also be necessary, unless a standard specification is considered acceptable. The blade angles are the most useful specifications, but may not be the most convenient, so there is provision to opt for choices such as camber angle, θ, stagger angle, γ or lift coefficient, C_{l0}. The program can then compute κ_1 and κ_2 from the data actually supplied, as described in Chapter 4. In the case of shrouded stator blades, the shroud seal clearance and the number of seal fins will also be required instead of the blade tip clearance. There are a number of features that can easily be incorporated to greatly simplify the blade geometry specification process, particularly for industrial axial-flow compressors. These include:

- The capability to copy the geometry of an already specified blade row.
- The capability to apply a geometrical scale factor to the data.
- The capability to impose a radial shift on the data.
- The capability to impose a change in stagger angle, i.e., to rotate the blade.
- The capability to import geometry from a file for a commonly used standard profile.
- The capability to export geometry to a file for use as a standard profile for future analyses.
- The capability to import geometry designed by the stage design procedure described in Chapter 10.

Often application of one or more of these procedures can greatly simplify the blade geometry input process so it requires at most, only minor editing, avoids the need to enter all data.

When conducting the actual performance analysis, the blade geometry on a stream surface is required. If the stream surface coordinates at the blade row inlet and discharge are (z_1, r_1) and (z_2, r_2), respectively, the stream surface angle, ϕ, is estimated from

$$\tan\phi = \frac{r_2 - r_1}{z_2 - z_1} \tag{9-1}$$

Then the corrected blade geometry on the stream surface is given by

$$c \rightarrow c / \cos\phi \tag{9-2}$$

$$t_b / c \rightarrow \cos\phi\, t_b / c \tag{9-3}$$

$$\tan\kappa_1 \rightarrow \cos\phi \tan\kappa_1 \tag{9-4}$$

$$\tan\kappa_2 \rightarrow \cos\phi \tan\kappa_2 \tag{9-5}$$

$$s = \pi(r_1 + r_2) / Z \tag{9-6}$$

Where base values are obtained from the input data by interpolation with respect to radius to obtain κ_1 at r_1, κ_2 at r_2, and other data at the mean radius. Then all other blade geometry data can be computed as described in Chapter 4.

9.2 CASCADE PERFORMANCE CONSIDERATIONS

Some care is required in applying and interpreting the empirical cascade performance models of Chapter 6 when predicting the performance of an axial-flow compressor. When analyzing a compressor at far off-design conditions, specific blade rows may operate locally in deep stall or in choke while other blade rows operate under near optimum conditions. If the empirical models of Chapter 6 are applied directly, the overall performance analysis will be very unreliable and incapable of analyzing many cases where the compressor is capable of operation. The major reason for this is that the meridional through-flow analysis of Chapter 7 does not permit any fluid mixing between stream sheets, such that entropy can build up locally on a stream surface to cause the solution to diverge. In the actual compressor blade rows, there are substantial secondary flow patterns or boundary layer migration, which does result in fluid mixing between stream sheets. Thus, it is necessary to impose limits on the loss coefficient models and apply some artificial smoothing procedures to simulate the fluid mixing processes. This writer imposes the following limit on all loss coefficients:

$$\overline{\omega} \le 0.5 \tag{9-7}$$

This will rarely be required, except when analyzing flow points where local choke is encountered in the blade passages. This can be encountered when the compressor is operating close to its choke limit and flow profiles are highly distorted. Smoothing of the total pressure loss is a more important consideration. Without it, the performance analysis can be very unreliable for predicting performance close to the surge line. This is particularly true at low off-design speeds, where severe local blade stall is commonly encountered. If N stream surfaces are used from hub to shroud, the total pressure loss on stream surface number i is given by

$$(\Delta P_t')_i = \overline{\omega}_i (P_{ti}' - P_i)_{in} \tag{9-8}$$

The prime designates the total pressure in a frame of reference relative to the blade row, and the subscript i designates the stream surface, numbered sequentially from the hub contour. Smoothed total pressure loss values are computed from

$$(\Delta P_t')_{i,c} = \left[(\Delta P_t')_{i-1} + 2(\Delta P_t')_i + (\Delta P_t')_{i+1}\right]/4;\ 1 < i < N \tag{9-9}$$

$$(\Delta P_t')_{1,c} = 2(\Delta P_t')_{2,c} - (\Delta P_t')_{3,c} \tag{9-10}$$

$$(\Delta P_t')_{N,c} = 2(\Delta P_t')_{N-1,c} - (\Delta P_t')_{N-3,c} \tag{9-11}$$

Equations (9-10) and (9-11) are derived from a simple trapezoidal-rule numerical approximation for the integral of the total pressure loss over the two stream sheets adjacent to the walls. They result in those integrals being identical when approximated using either the smoothed or the uncorrected total pressure loss values at those three points.

9.3 STALL AND COMPRESSOR SURGE CONSIDERATIONS

An important consideration in performance analysis is estimating the compressor's surge limit from the detailed performance data. This is rather subjective and imprecise, but there are some useful indicators that have been found to be helpful in this process. It is well known that a pressure versus flow characteristic at constant speed, which has a positive slope, is theoretically unstable. Hence, a predicted characteristic that approaches a slope of zero can be considered to be an obvious indication of probable surge. But in most cases, the performance analysis will not be capable of resolving the characteristic's slope accurately enough to rely on this. Indeed, the occurrence of a positive slope is often not even obvious from experimental performance data. In the presence of blade or end-wall boundary layer stall, there may be a very abrupt drop in compressor discharge pressure that is not apparent from either the predictions or experiment. Of course, in the case of the predictions, this lack of resolution is really deliberate. Practices such as the loss smoothing previously discussed are employed to achieve acceptable reliability, which will preclude resolving any abrupt changes in performance due to the onset of local stall. The best we can do is attempt to identify stall parameters that may indicate such an abrupt change is likely to occur.

Blade stall is expected to be a function of the limit loading diffusion factors, such as D or D_{eq} of Chapter 6. In this writer's experience, those parameters are of limited value as a means of estimating stall limits likely to be associated with the compressor's surge limit. It is quite common to observe values of these diffusion factors well in excess of typical recommended loading limits at operating points well removed from the observed surge line. A stall criterion proposed by de Haller (1953) is given by

$$W_2 / W_1 < 0.72 \tag{9-12}$$

The generally accepted opinion today is that de Haller's criterion is associated with an end-wall stall rather than a blade stall. In any event, this criterion has been found to be more effective than the diffusion factors as an indicator of the onset of surge. But, again, a significant number of exceptions are encountered where velocity ratios well below this limit are predicted at operating points that are quite far from a compressor's surge limit. Koch (1981) improved on the simple de Haller criterion by including blade geometry parameters. Koch approximated the blade passages, averaged over a stage, as a simple diffuser. He was able to achieve reasonable agreement between observed stage pressure coefficients at stall with the two-dimensional diffuser data of Sovran and Klomp (1967) for a specific inlet blockage level. To obtain this correlation, the compressor stage data was extensively corrected to adjust for differences in blade clearance, Reynolds number and axial spacing between blade rows. This correlation is intended as a means to estimate the maximum achievable stage pressure coefficient. It is of limited value as a stall criterion for use in an axial-flow compressor performance analysis. Here, a stall criterion for a blade row instead of a stage is needed. The use of pressure coefficient is also undesirable, since it results in a stall criterion that is a strong function of the blade performance models, which are by no

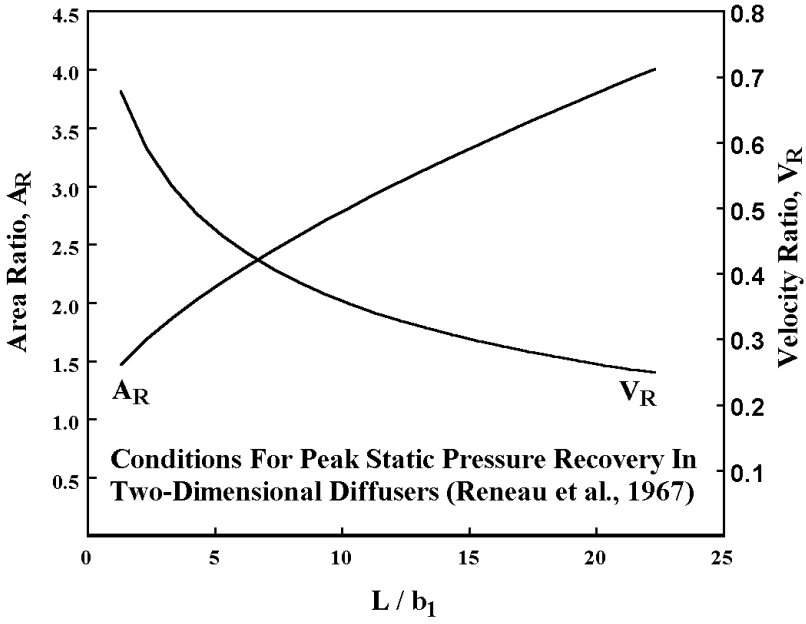

FIGURE 9-2 Two-Dimensional Diffuser Correlation

means universal methods. Finally, the Koch correlation requires a number of corrections for it to be applicable to a specific axial-flow compressor.

This writer has developed a correlation for the onset of stall that is more appropriate to the present application. Reneau et al. (1967) developed a graphical correlation for the geometry of simple two-dimensional diffusers operating at their peak static pressure recovery. Aungier (2000) correlated their data in the form

$$A_R = 1 + 0.4(L / b_1)^{0.65} \tag{9-13}$$

Where A_R is the diffuser area ratio, L is the diffuser length and b_1 is the diffuser width at the inlet. Since the diffuser test data correspond to basically incompressible flow, this can also be related to the ideal diffuser velocity ratio, V_R.

$$V_R = 1 / [1 + 0.4(L / b_1)^{0.65}] \tag{9-14}$$

Equations (9-13) and (9-14) are presented in Fig. 9-2. Note that these equations identify peak pressure recovery condition, but are not dependent on the value of the peak pressure recovery. It is reasonable to expect the onset of stall in any diffusing passage to closely correspond to this peak pressure recovery condition. To apply this concept to a blade passage, it is assumed that L should be the camberline

length and b_1 should be the staggered spacing. If the camberline is approximated as a circular-arc, this can be written as

$$L / b_1 \rightarrow L / g = L / (s \cos \gamma) = \theta \sigma / [2 \sin(\theta / 2) \cos \gamma] \tag{9-15}$$

When applying an incompressible flow model to compressible flow through a blade row, it is always preferable to employ velocity pressures rather than velocity to minimize the influence of Mach number effects, i.e.,

$$V_R \rightarrow W_{RE} = \sqrt{\frac{P'_{t2} - P_2}{P'_{t1} - P_1}} \tag{9-16}$$

W_{RE} will be called the equivalent relative velocity ratio across the blade row. Hence the expected stall criterion is

$$W_{RE} < \frac{(0.15 + 11 t_b / c) / (0.25 + 10 t_b / c)}{1 + 0.4[\theta \sigma / [2 \sin(\theta / 2) \cos \gamma]]^{0.65}} \tag{9-17}$$

The numerator on the right-hand side of this equation reflects a very weak dependence on the ratio of t_b/c observed while comparing stall estimates from Eq. (9-17) with observed axial-flow compressor surge limits. These comparisons have also suggested two other modifications: First, the application to blade passages requires extrapolating Eq. (9-14) to values of L / b_1 that are considerably lower than those covered by the test data and correlation of Reneau et al. (1967). Thus, a limit is imposed on the effective value of L/b_1 used on the right-hand side of Eq. (9-17) by requiring

$$\theta \sigma / [2 \sin(\theta / 2) \cos \gamma] \geq 1.1 \tag{9-18}$$

Second, Eq. (9-17) can be too pessimistic for highly diffusing blades, where blade wake blockage can be expected to be significant. It is rather subjective and very tedious to attempt to estimate stall in those cases. It has been observed that Eq. (9-17) becomes pessimistic whenever D_{eq} is greater than about 2.2. When $D_{eq} > 2.2$, an empirical correction to Eq. (9-17) has been found to be reasonably effective, i.e.,

$$W_{RE} < \frac{[(2.2 / D_{eq})^{0.6}](0.15 + 11 t_b / c) / (0.25 + 10 t_b / c)}{1 + 0.4[\theta \sigma / [2 \sin(\theta / 2) \cos \gamma]]^{0.65}} \tag{9-19}$$

The stall criterion for $D_{eq} < 2.2$ and $t_b / c = 0.1$ is illustrated in Fig. 9-3.

In summary, this writer employs the following three basic criteria as a basis for estimating the onset of compressor surge:

1. When the discharge pressure versus flow characteristic approaches a slope of zero.
2. When end-wall boundary layer stall is predicted ($H_1 = 2.4$).
3. When stall is indicated by Eqs. (9-17) through (9-19).

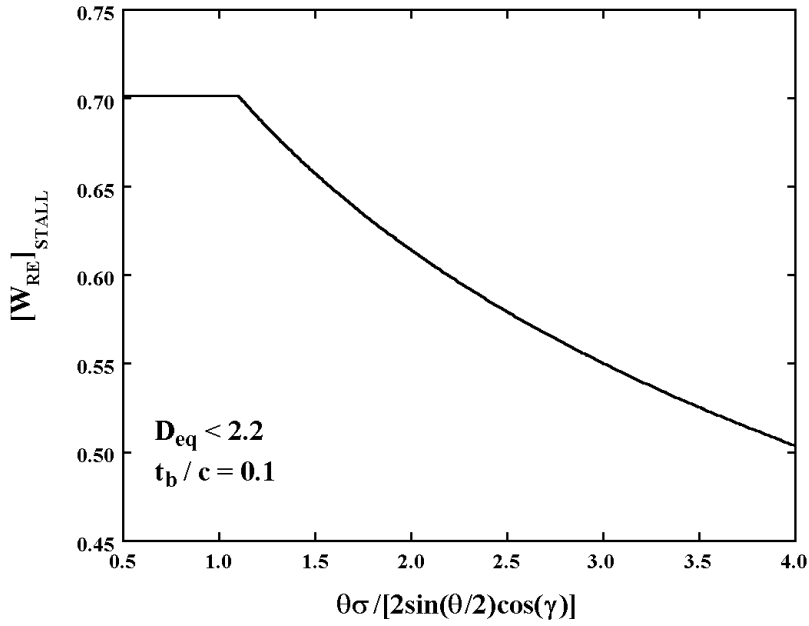

FIGURE 9-3 The Blade Row Stall Criterion

The first two criteria are employed at all speeds, while the third criterion is most reliable for speeds greater than about 85% of design speed. At lower speeds, the flow profiles typically become so distorted that the accuracy of the profile predictions with the inviscid through-flow analysis of Chapter 7 becomes too questionable for it to rely heavily on the third criterion. This will be illustrated in the presentation of results from the performance analysis.

9.4 APPROXIMATE NORMAL EQUILIBRIUM RESULTS

The approximate normal equilibrium model described in Section 7.6 offers substantial advantages in computation speed and reliability over the full normal equilibrium method. This approximation assumes that the stream surface slope and curvature vary linearly between the two known end-wall contours. In this section, typical results from the performance prediction procedures described in this book using the approximate normal equilibrium model will be reviewed. In the next section, results for the same problems using the full normal equilibrium model will be reviewed for comparison.

Figure 9-4 compares performance predictions with experiment for the NACA 10-stage subsonic axial-flow compressor. The compressor design is described in Johnsen (1952). The performance data are provided in Budinger and Thomson

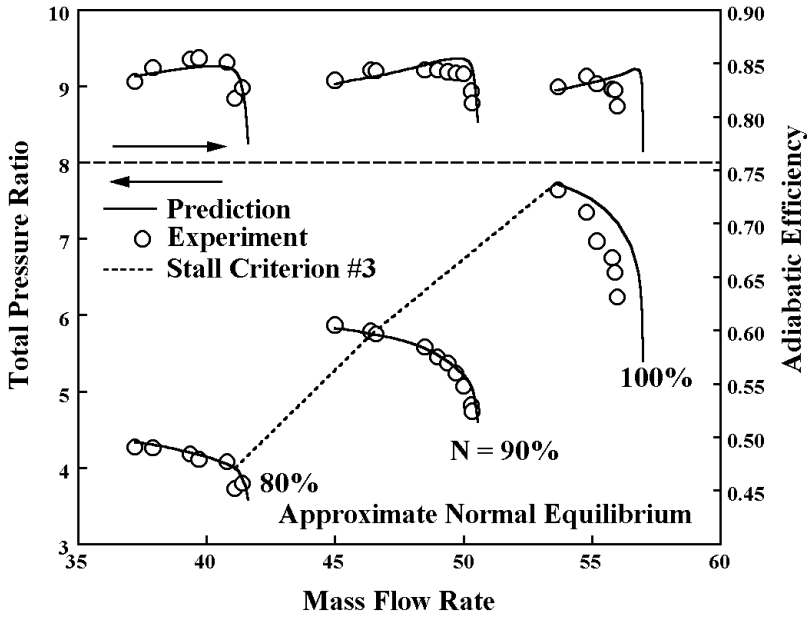

FIGURE 9-4 The NACA 10-Stage Compressor

(1952). All blade rows in this compressor use fairly conventional NACA 65-series blades. Design data for the inlet guide vane are not provided in the references, so the performance analysis was started at a station downstream of the inlet guide vane using experimental measurements of the flow angle distribution, with an assumed end-wall boundary layer blockage of 2%. Typical end-wall boundary layer blockage predictions for this case were shown in Fig. 8-8. The estimated stall line based on stall criterion #3 is also shown in Fig. 9-4. The experimental compressor surge limit is well approximated by the lowest flow data point for each speed line. It is seen that stall criterion #3 is a good indicator of surge at the design speed, but is pessimistic at lower speeds, where stall criterion #1 is the best indicator. This compressor has the unusual characteristic that stall criterion #3 is first encountered in the front stages at the rotor tips and that the limit expressed in Eq. (9-18) is active at these locations. Under these conditions, stall criterion #3 is of questionable validity and it is far too insensitive to variations in mass flow rate to be very useful. At the tips of the front stage rotors of an axial-flow compressor, the variation of W_{RE} with mass flow rate is far too weak to resolve a meaningful stall limit. For example, the difference in W_{RE} between the experimental and predicted surge limits at 90% speed is just 0.015. This is the only axial-flow compressor encountered by this writer with this unusual characteristic. It is normally the case that blade diffusion limits are first encountered along the hub contour, where W_{RE} shows the strongest variation with mass flow rate. Flow diffusion limits are easier to avoid at the rotor tips, and designers

have strong incentive to do so due to the higher Mach number levels encountered there.

Figure 9-5 compares performance predictions with experiment for the NACA 5-stage transonic axial-flow compressor (Kovach and Sandercock, 1961). Sandercock et al. (1954) describes the detailed design. Kovach and Sandercock (1954) provide the experimental performance data. The first two stator rows and all rotor rows in this compressor use double-circular-arc blades, while the last three stator rows use NACA 65-series blades. This case provides a fairly significant test of all high Mach number performance models used, including bow-shock losses, supercritical Mach number effects and blade passage choking. This analysis was started well up in the inlet passage with negligible inlet end-wall boundary layer blockage. Figure 9-1 illustrates the compressor cross-section and the computational stations used in this analysis. Typical end-wall boundary layer blockage predictions for this case were shown in Fig. 8-9. The estimated stall line from stall criterion #3 is also shown in Fig. 9-5. The experimental compressor surge limit is not well defined in the references, but presumably can be approximated by the lowest flow data point on a speed line. At 90% and 100% speed, there is substantial scatter in the experimental data, so the surge limit is less obvious and possibly better indicated by the highest pressure-ratio point achieved on the speed line. It is seen that stall criterion #3 is reasonably significant as an indicator of surge at all speeds. This case provides a fairly dramatic illustration of the merits of stall criterion #3, as shown in Fig. 9-6. The predicted equivalent velocity

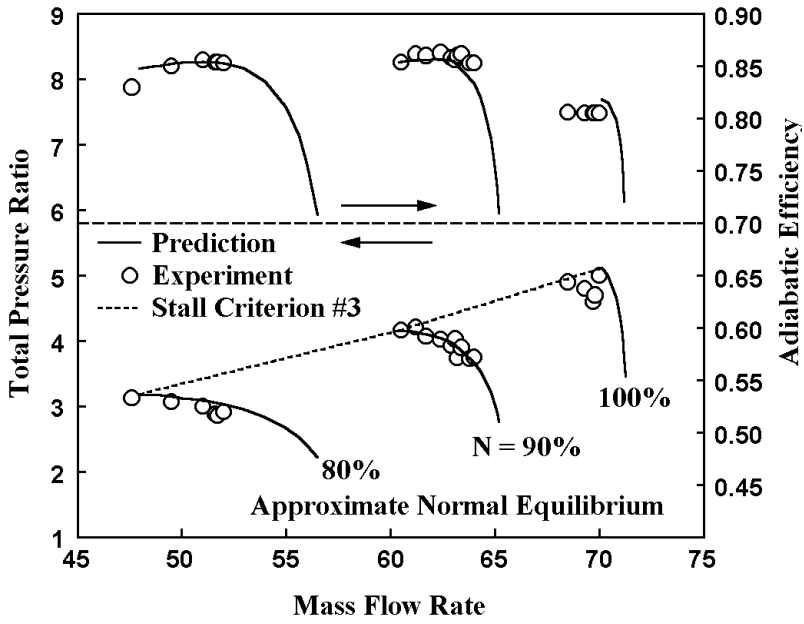

FIGURE 9-5 The NACA 5-Stage Compressor

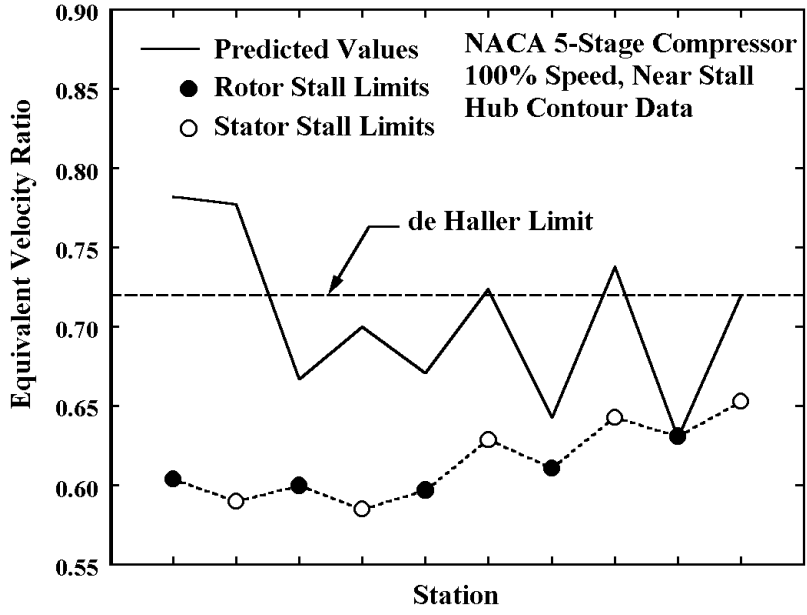

FIGURE 9-6 Illustration of Stall Criterion 3

ratios defined by Eq. (9-16) along the hub contour are shown for all blade rows, along with the stall limit values computed from Eqs. (9-17) through (9-19). The simple de Haller limit of Eq. (9-12) is also shown for reference. It is apparent that the simple de Haller limit would predict a substantially lower pressure ratio at stall. Indeed, the de Haller criterion predicts that blade stall is present for the entire predicted characteristic shown in Fig. 9-5. For the specific blade geometry used in this compressor, Eqs. (9-17) through (9-19) predict a stall limit well below the de Haller limit. Although an unusually extreme example, this case serves to demonstrate the importance of a more fundamental stall criterion than that proposed by de Haller.

Figure 9-7 compares performance predictions with experiment for the NACA 8-stage transonic axial-flow compressor (Voit, 1953; Geye et al., 1953). The first two rotor blade rows use double-circular-arc blades. All other blade rows use NACA 65-series blades. The performance analysis for this case is a little less precise than the previous examples. The hub contour around the first stator row is not well defined in Voit (1953) and the exit guide vane row geometry is not supplied. The exit guide vane is not expected to have a significant influence on the total-to-total pressure ratio prediction. So an exit guide vane was simply designed for this compressor for use in the performance analysis. The exit guide vane design used a blade configuration similar to that of the last stator row, with camber and stagger angles defined to effectively remove the swirl from the flow exiting the last stator row. The analysis was started well upstream in the inlet passage

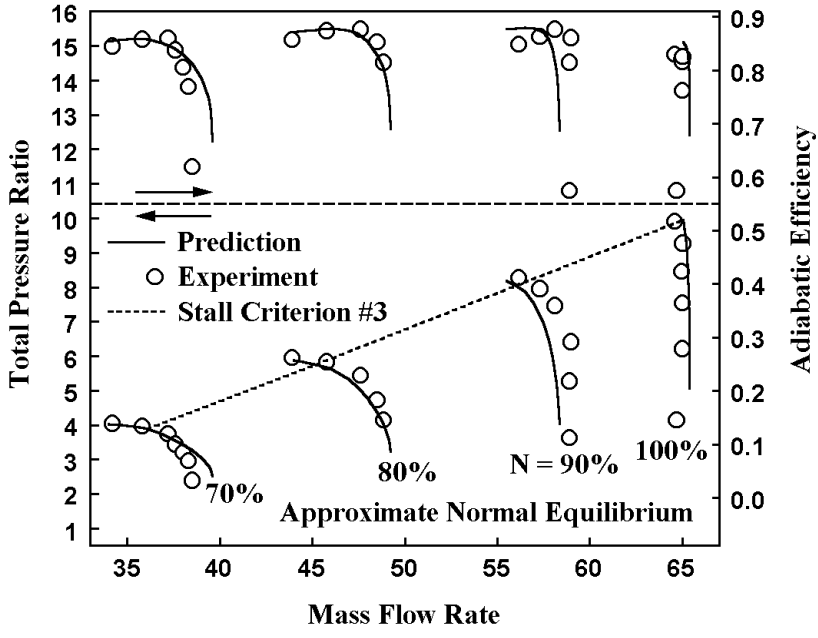

FIGURE 9-7 The NACA 8-Stage Compressor

with negligible inlet end-wall boundary layer blockage. Typical end-wall boundary layer blockage predictions for this case were shown in Fig. 8-7. The estimated stall line from stall criterion #3 is also shown in Fig. 9-7. The experimental compressor surge limit is well approximated by the lowest flow data point for each speed line (Geye et al., 1953). Stall criterion #3 is a good indicator of the surge limit at the 90% and 100% speed lines, but is somewhat conservative at the 70% and 80% speed lines, where stall criterion #1 is a better indicator.

9.5 FULL NORMAL EQUILIBRIUM RESULTS

Figures 9-8 through 9-10 compare performance predictions using the full normal equilibrium model with the approximate normal equilibrium results from the previous section. Except for some minor differences in the stall lines estimated from the two models, it is seen that the performance predictions from the two models are essentially identical. It is quite evident that there is very little loss in performance prediction accuracy when the approximate normal equilibrium model is used for these three compressors. This is quite typical of this writer's experience on other axial-flow compressor performance analyses. There is almost never a need to employ the full normal equilibrium model to obtain accurate overall compressor performance predictions.

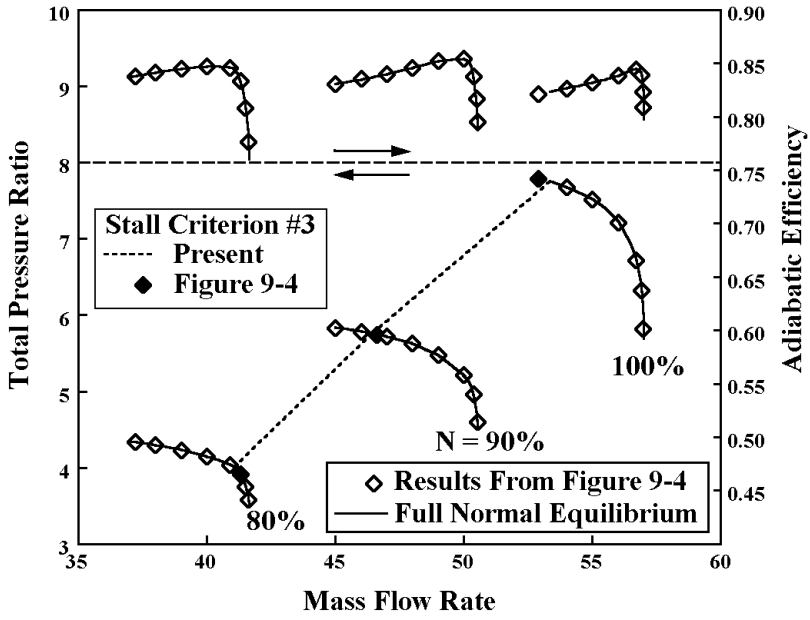

FIGURE 9-8 The NACA 10-Stage Compressor

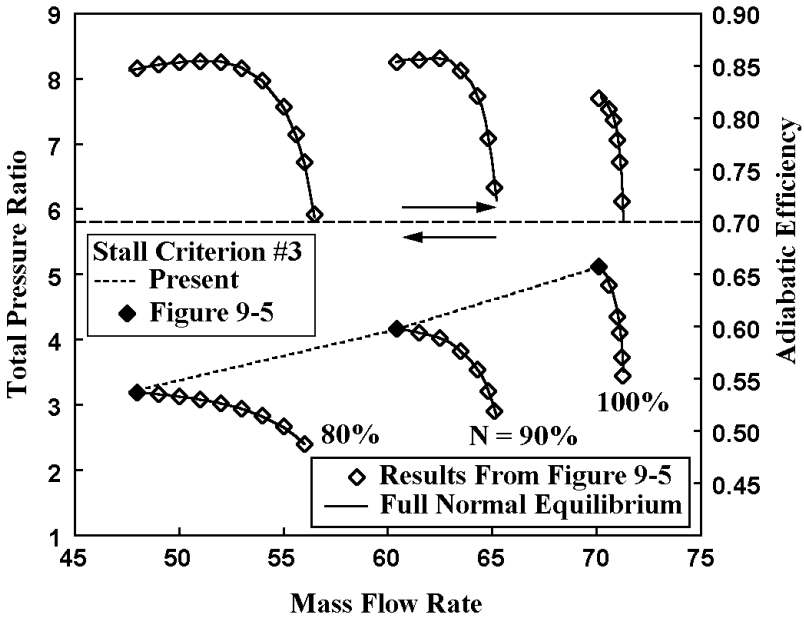

FIGURE 9-9 The NACA 5-Stage Compressor

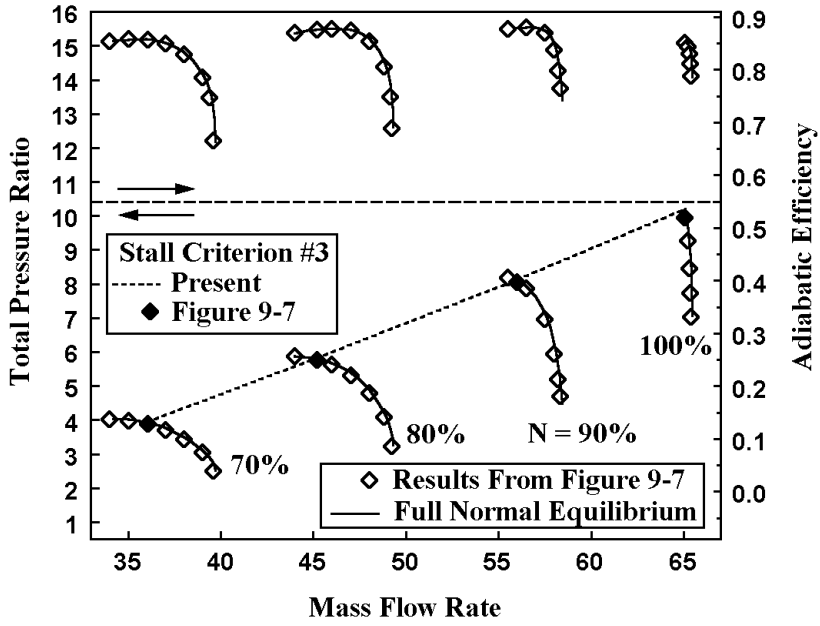

FIGURE 9-10 The NACA 8-Stage Compressor

9.6 CONCLUDING REMARKS

This chapter provides supplemental procedures to apply the analyses described in Chapters 6 through 8 to the prediction of the aerodynamic performance of axial-flow compressors. The resulting performance analysis has been applied to three NACA axial-flow compressors to demonstrate the level of prediction accuracy to be expected. The compressors considered cover a significant variety of design styles, ranging from the conservative subsonic NACA 10-stage compressor to the more aggressive transonic designs used in the NACA 5-stage and 8-stage compressors. But it must be recognized that the empirical models of Chapter 6 specifically cover only the convention blade profiles of Chapter 4. Application of these procedures to other blade profiles, such as proprietary controlled diffusion airfoils, may require supplemental empirical performance models to achieve the same level of prediction accuracy as demonstrated by the results provided in this chapter.

The performance predictions reviewed in this chapter show that the approximate normal equilibrium model of Section 7.6 provides excellent prediction accuracy as well as dramatic improvements in computation speed and reliability. This supports an earlier comment in this chapter suggesting that one-dimensional mean-line performance analysis methods no longer offer any significant advantage over the more fundamental hub-to-shroud flow performance analyses.

Some general guidelines have been suggested for estimating a compressor's surge limit based on the performance analysis results. These guidelines can

normally be refined and improved through comparison with experimental results when the analysis is applied to user-specific design styles and blade profile types. Surge is a transient phenomenon dependent upon the complete system in which the compressor operates. Consequently, the surge limit cannot be predicted by a compressor performance analysis. A performance analysis can only provide fluid dynamic data that may be used as a guide to estimate the probable surge limit. It should be apparent from the results presented in this chapter that this process remains quite subjective, relying heavily on the experience and judgment of the aerodynamicist to interpret results from the performance analysis. At speeds close to the design speed, the stages are reasonably well matched. In these cases, stall criterion #3 is usually the best indicator. At speeds much less than the design speed, excessive front stage loading produces severe flow profile distortion, making the predicted values of W_{RE} too inaccurate for stall criterion #3 to be very useful. There, stall criterion #1 is the most useful indicator. Although stall criterion #2 isn't a factor in the cases considered in this chapter, it is occasionally encountered. There is evidence to suggest that stable operation is very unlikely when significant end-wall boundary layer separation is predicted. In the few cases encountered, stall criterion #2 provided a good estimate of the surge limit and none of those compressors actually operated beyond that limit.

EXERCISES

9.1 Show that the integration of the corrected total pressure loss data from Eqs. (9-9) and (9-10) with respect to mass flow rate between stream surfaces 1 and 3 yields the same result as integration of the uncorrected total pressure loss data. Assume the mass flow rate is identical in all stream sheets and equal to $\Delta\dot{m}$. Use the simple trapezoidal rule approximation for numerical integration, e.g.,

$$\int_0^{\Delta\dot{m}} \Delta P_t' d\dot{m} \approx \tfrac{1}{2}[(\Delta P_t')_1 + (\Delta P_t')_2]\Delta\dot{m}$$

9.2 Derive an expression for the ratio of the blade camberline length-to-the staggered spacing, $s\cos\gamma$, for a circular-arc camberline to confirm Eq. (9-15).